

Syntheses and characterization of Schiff-base ligand complexes of nickel (II) with different nuclearity and studies of their catecholase activity

Averi Guha

Assistant Professor, Dept. of Chemistry, Surendranath Evening College, Kolkata

Abstract—two novel nickel(II) complexes, formulated as $[\text{Ni}_2\text{L}^1_2(\text{H}_2\text{O})_4(\text{NO}_3)_2]$ (1) and $[\text{Ni}_5\text{L}^2_2(\text{OAc})_6(\text{OH})_2] \cdot 5.5\text{H}_2\text{O}$ (2), have been synthesised and structurally characterised by X-ray crystallographic study, where L^1 and L^2 represent 2-formyl-4-methyl-6-(1-(2-aminomethyl)piperidine)-iminomethylphenolato and 4-methyl-2,6-bis(1-(2-aminomethyl)piperidine)-iminomethylphenolato ligand, respectively. One pot reaction between 2,6-diformyl-4-methylphenol with 1-(2-aminoethyl) piperidine, in presence of nickel (II) nitrate and nickel (II) acetate salt, afforded in situ [1+1] and [1+2] condensation leading to Schiff-bases HL^1 and HL^2 , and to complexes 1 and 2 of different nuclearity, respectively. Both processes were conducted maintaining the same reaction conditions in anhydrous EtOH. The preferential attainment of bi- or pentanuclear compounds seems mediated by the anion of the Ni(II) salt used. Complex 1 is formed by two unsymmetrical tridentate ligands L^1 chelating in a head-tail fashion the metal ions to make a centrosymmetric phenoxido-bridged Ni(II) dimer. Two water molecules complete the octahedral coordination of the metal ions. Conversely in complex 2 two $[\text{Ni}_2(\text{OAc})\text{L}^2]^+$ units, having a syn-syn bidentate bridging acetate, embrace a third Ni atom through bridging acetate and μ_3 -hydroxyl anions, giving rise to an adduct of C_2 symmetry where the compartmental ligand planes form a dihedral angle of ca. 82° . The catecholase activity of these complexes were explored, and both the complexes showed to effectively catalyze the conversion of 3,5-di-tert-butylcatechol (3,5-DTBC) to 3,5-di-tert-butylbenzoquinone (3,5-DTBCQ).

I. INTRODUCTION

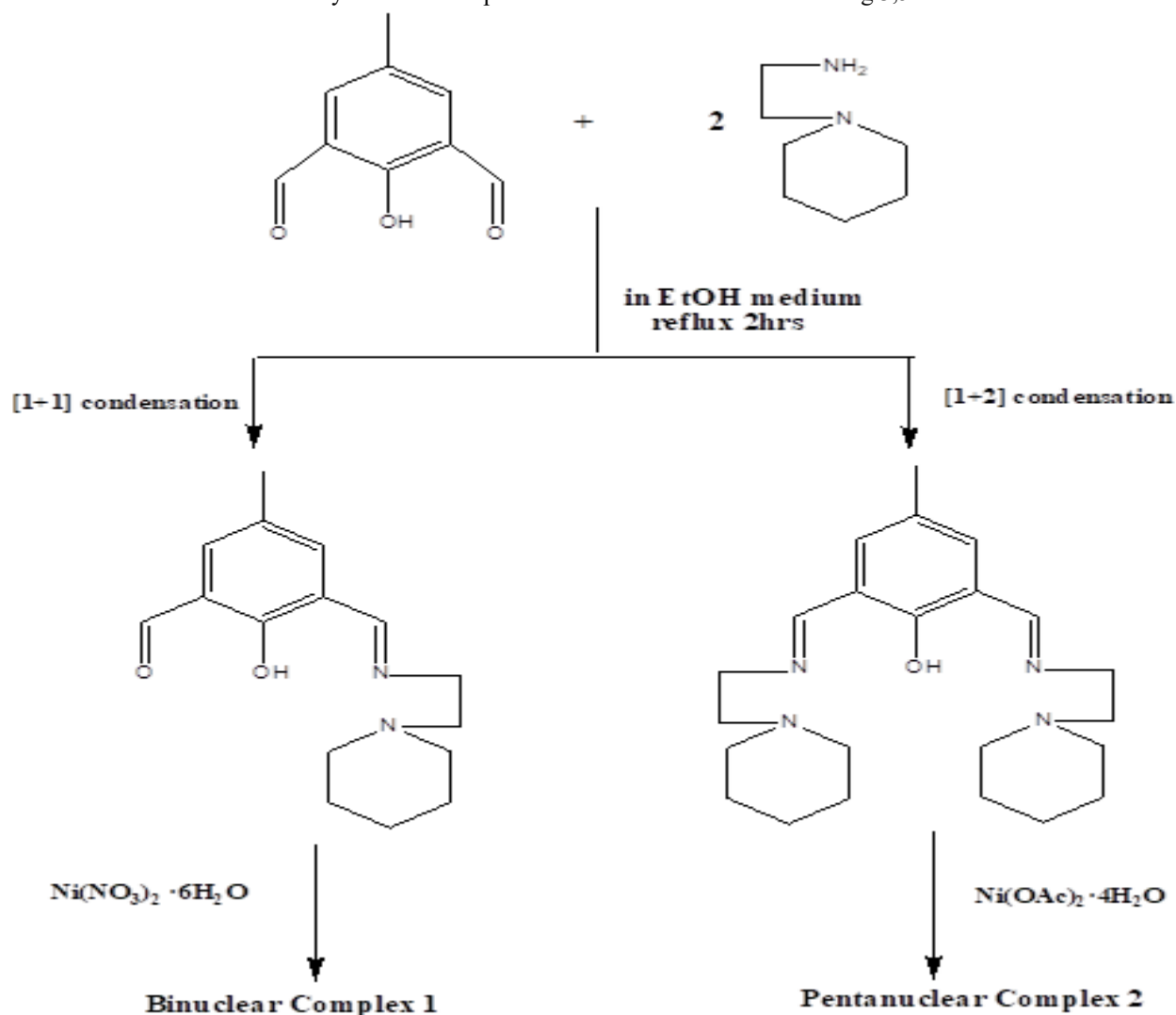
Transition metal complexes with two or several metal ions in close proximity are of considerable interest as models of active centers of metal-containing proteins, molecular magnets, and potential components of homogeneous catalytic systems [1-9]. Multinuclear transition and rare earth metal complexes also have

attracted extensive interest for their unusual behavior such as the multielectron redox reactivity for substrates and ferromagnetic or antiferromagnetic properties [10-13]. Recent years have witnessed an explosion of interest in the design, synthesis and potential application in material science of polynuclear molecules and molecule-based coordination polymers of different dimensionality [21-23].

Despite the interest in the properties of such complexes, synthetic methods have yet to reach the level of efficiency attained with mononuclear complexes. However, the synthesis of polynuclear complexes requires an appropriate choice of ligand systems and Schiff-base ligands may serve this purpose. Generally, Schiff-base formation depends on the nature of the amine, the carbonyl moiety and of their relative stoichiometry. Although polynuclear Ni clusters with acetate, [24,25] perchlorate [26] or azido anions.[27] have been described, no report put emphasis on the catalytic influence of the metal salt used. Here we report in situ formation of 1+1 and 1+2 condensed Schiff-bases starting from 2,6-diformyl-4-methylphenol and 1-(2-aminoethyl) piperidine mediated by acetate or nitrate Ni(II) salts and on the corresponding di- and penta-nuclear metal complexes. The syntheses (**Scheme 1**) were conducted with an one-pot template condensation reaction in anhydrous EtOH. Surprisingly it was observed that, by using nickel(II) nitrate, a [1+1] Schiff-base condensation takes place along with the formation of a binuclear complex. Whereas nickel(II) acetate lead to a [1+2] condensation between the precursors giving origin to a pentanuclear complex. We have also tried with other anions, such as SO_4^{2-} , Cl^- , and PO_4^{3-} , etc. but no solid products can be

isolated. The catecholase activity of these complexes

were also studied using 3,5-DTBC as substrate.



Scheme 1. Synthetic out-line of the Schiff-base ligands and their nickel(II) complexes.

II. RESULTS AND DISCUSSION

Syntheses

Complex **1** is prepared by applying template synthesis technique treating nickel(II) nitrate hexahydrate with the Schiff-base formed *in situ* between 2,6-diformyl-4-methylphenol and 1-(2-aminoethyl) piperidine in anhydrous ethanol. Complex **2** is prepared following same procedure as for **1** by using nickel(II) acetate tetrahydrate instead. The ratio of diformyl, amine and nickel(II) salt was maintained as 1 : 2 : 2.5.

Characterization

(i) Infrared Spectra

Infrared spectra for all complexes were collected in the range 4000-400 cm^{-1} . The spectra of the complexes **1** and **2** are shown in Figures 1 and 2. Complexes **1-2** show bands in IR spectra at 1639 cm^{-1} due to C=N stretching and skeletal vibration in the range 1543-1591 cm^{-1} . Complex **1** exhibits band at 1384 cm^{-1} due to NO_3^- groups [28]. Complex **2** shows a band centred around 1037 cm^{-1} due to the acetate anions.

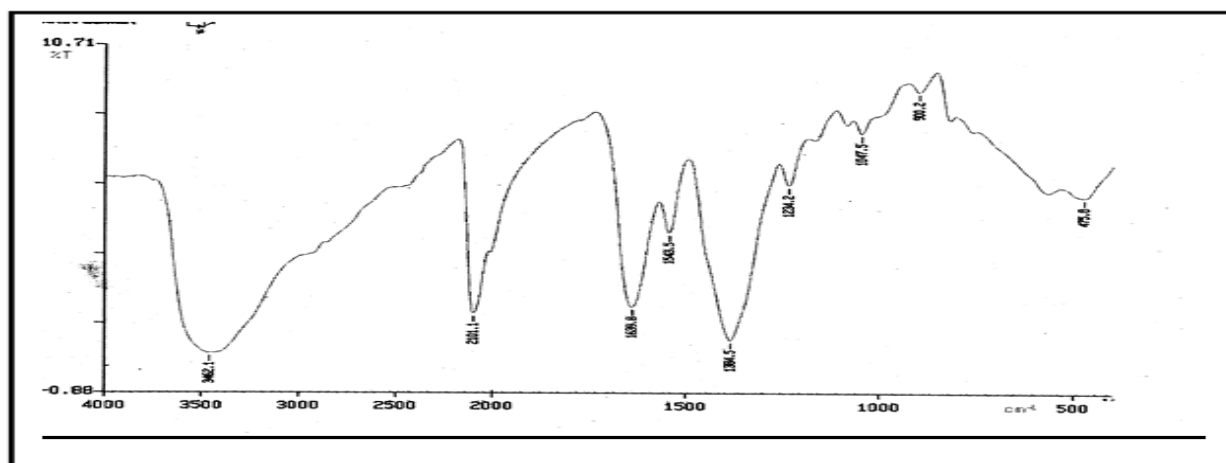


Figure 1 IR spectrum of complex 1.

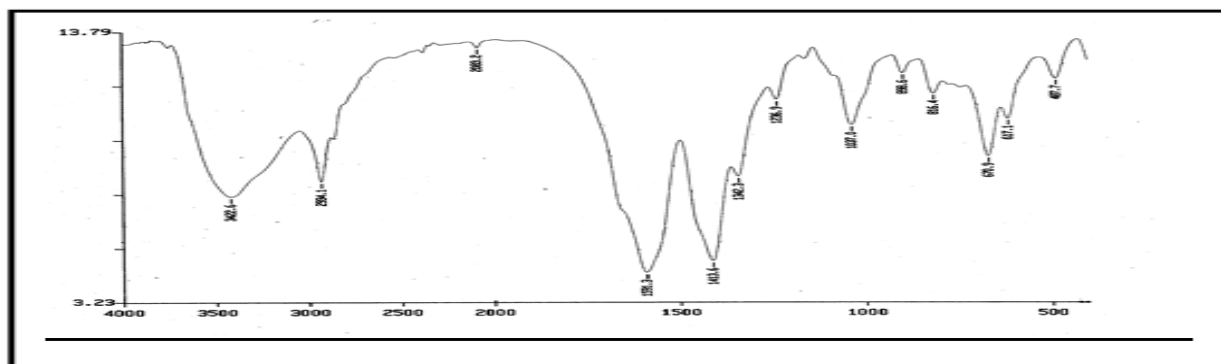


Figure 2 IR spectrum of complex 2.

(ii) Electronic Spectra

In general, Ni^{II} complexes having octahedral coordination environment show three spin allowed d-d transitions in the ranges 1250 - 900 (${}^3\text{A}_{2g} \rightarrow {}^3\text{T}_{2g}$), 670 - 520 (${}^3\text{A}_{2g} \rightarrow {}^3\text{T}_{1g}(\text{F})$), and 500 - 370 (${}^3\text{A}_{2g} \rightarrow {}^3\text{T}_{1g}(\text{P})$) nm with low molar absorptivity coefficients ($< 30 \text{ mol L}^{-1} \text{ cm}^{-1}$) [29]. The electronic spectra of complexes **1** and **2** are typical for octahedral high-spin nickel(II) ion [30]. The electronic spectra of both the complexes show three characteristic peaks corresponding to octahedral $\text{Ni}(\text{II})$ species as given in Figures 3 & 4.

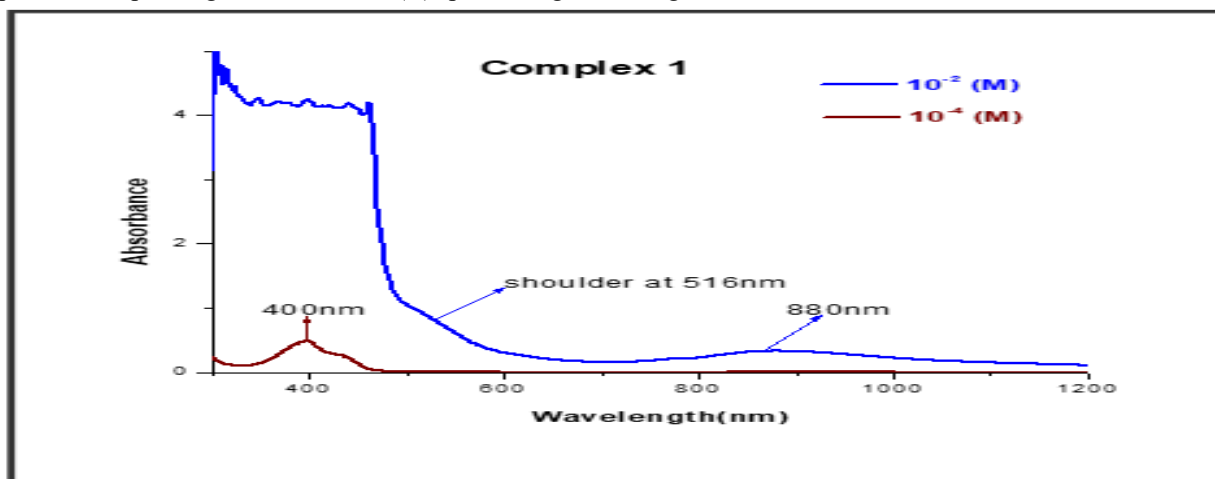


Figure 3 The electronic spectra of complex 1 in methanol at different concentrations.

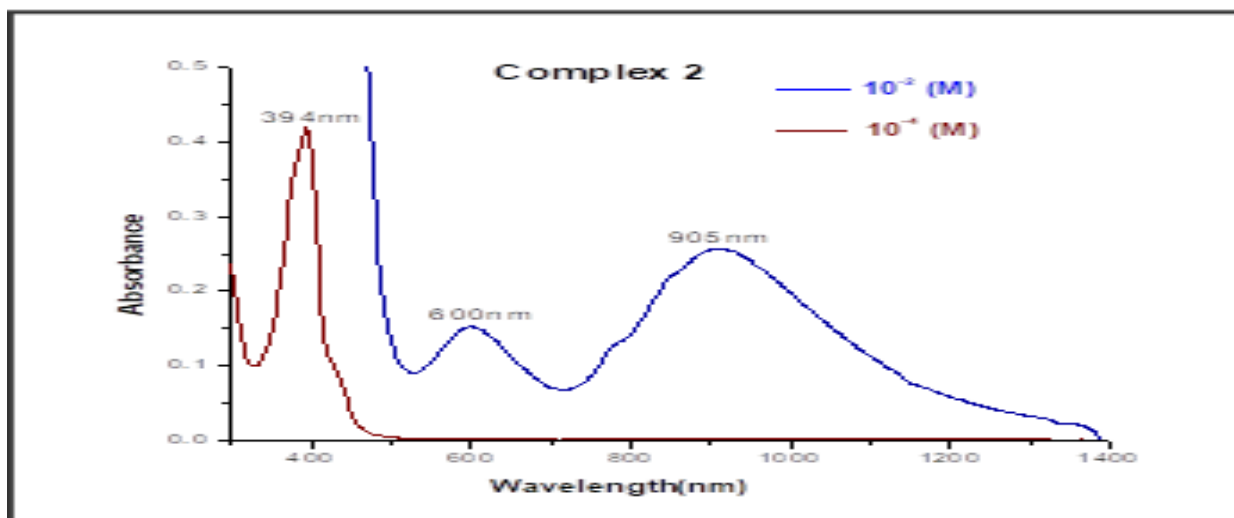


Figure 4 The electronic spectra of complex 2 in methanol at different concentrations.

Description of crystal structures

The crystal structure analysis of complex 1 reveals a dinuclear complex cation and nitrate anions. The complex, located on a crystallographic inversion center, is formed by two unsymmetrical tridentate ligands that chelate the metal ions in a head-tail arrangement, and create a phenoxido-bridged Ni(II) dimer. An ORTEP view of the complex cation of 1 with atom labeling scheme of the independent part is shown in Figure 5 and a selection of bond lengths and angles is given in Table 1. The metals, separated by 3.0702(7) Å, exhibit an octahedral coordination sphere, with two phenoxido-bridged oxygens, an

imine nitrogen donor and a carbonyl oxygen, completing the coordination sphere through two water molecules at axial positions. The complex has coplanar phenol moieties with pyperidine rings (showing a chair conformation) far away from the metal center. The Ni-N and Ni-O bond distances in the equatorial plane are comparable in length ranging from 2.004(2) to 2.023(2) Å, whereas the aqua ligands reside at slightly longer distances, of 2.086(2) and 2.092(2) Å. The crystal packing shows nitrate anions H-bond connected to water molecules (O...O distance of ca 2.78 Å) forming 2D layers parallel to crystallographic planes (100) (Figure 6).

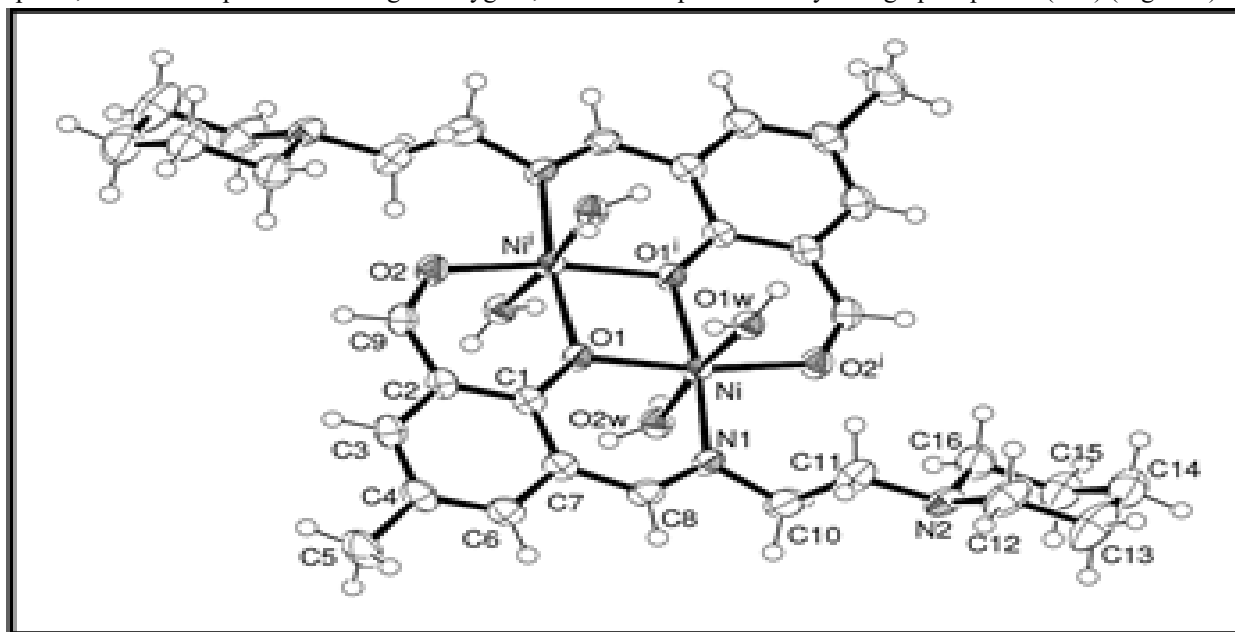


Figure 5 ORTEP drawing (50% probability ellipsoid) of the molecular cation of 1

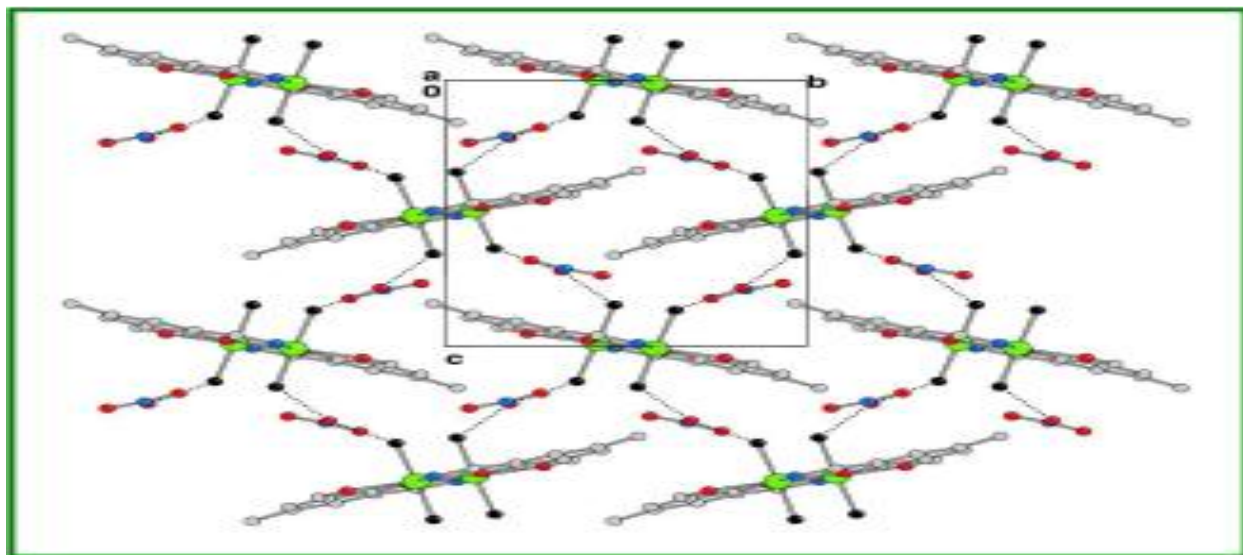


Figure 6 Crystal packing of complex 1: 2D network formed by H-bonds interactions occurring between aqua ligands and nitrate anions (piperidine rings not shown for sake of clarity).

Table 1 Selected bond lengths (Å) and angles (°) for complex 1.

Ni-O(1)	2.004(2)	Ni-N(1)	2.015(2)
Ni-O(1')	2.023(2)	Ni-O(1w)	2.086(2)
Ni-O(2')	2.016(2)	Ni-O(2w)	2.092(2)
O(1)-Ni-N(1)	91.34(10)	O(2')-Ni-O(1w)	88.51(9)
O(1)-Ni-O(2')	169.42(9)	O(1')-Ni-O(1w)	92.77(9)
N(1)-Ni-O(2')	99.21(10)	O(1)-Ni-O(2w)	92.73(9)
O(1)-Ni-O(1')	80.65(9)	N(1)-Ni-O(2w)	85.96(10)
N(1)-Ni-O(1')	171.86(10)	O(2')-Ni-O(2w)	88.82(9)
O(2')-Ni-O(1')	88.82(9)	O(1')-Ni-O(2w)	92.95(9)
O(1)-Ni-O(1w)	90.95(9)	O(1w)-Ni-O(2w)	173.63(9)
N(1)-Ni-O(1w)	88.77(10)	Ni-O(1)-Ni'	99.35(9)

Primed atoms $-x+2, -y, -z+1$.

In complex 2 the pentanuclear species can be described as formed by two $[\text{Ni}_2(\text{OAc})\text{L}^2]$ units connected to a third Ni center through bridging acetate and μ_3 hydroxyl anions (Figure 7) and a selection of bond lengths and angles is given in Table 2. All the three independent Ni ions present a distorted octahedral geometry with a different chromophore. In fact Ni(1) has a $\{\text{O}_5\text{N}\}$ coordination sphere provided by a μ_3 -OH, the bridging phenolato-O atom, three acetato-O atoms and an imino-N donor. Ni(2) is in $\{\text{O}_4\text{N}_2\}$ donor compartment

provided by a μ_3 -OH, the bridging phenolato-O atom, two acetato-O atoms, and the chelating amino- and imino-N atoms. The central Ni(3) atom is 6-coordinate ($\{\text{O}_6\}$ donor set) through two μ_3 -hydroxo groups and four oxygen from bridging acetate anions. The central Ni atom resides on a crystallographic two fold axis with the compartmental ligands that form a dihedral angle of $82.4(1)^\circ$. Two of the acetate linkers connecting Ni(3) with the $[\text{Ni}_2(\text{OAc})\text{L}^2]$ fragments act as *syn-syn* bidentate bridging and two as $\eta^2\mu_3$ triply bridging ligands (operative inside the convex angle formed by phenolato rings of Figure 8)

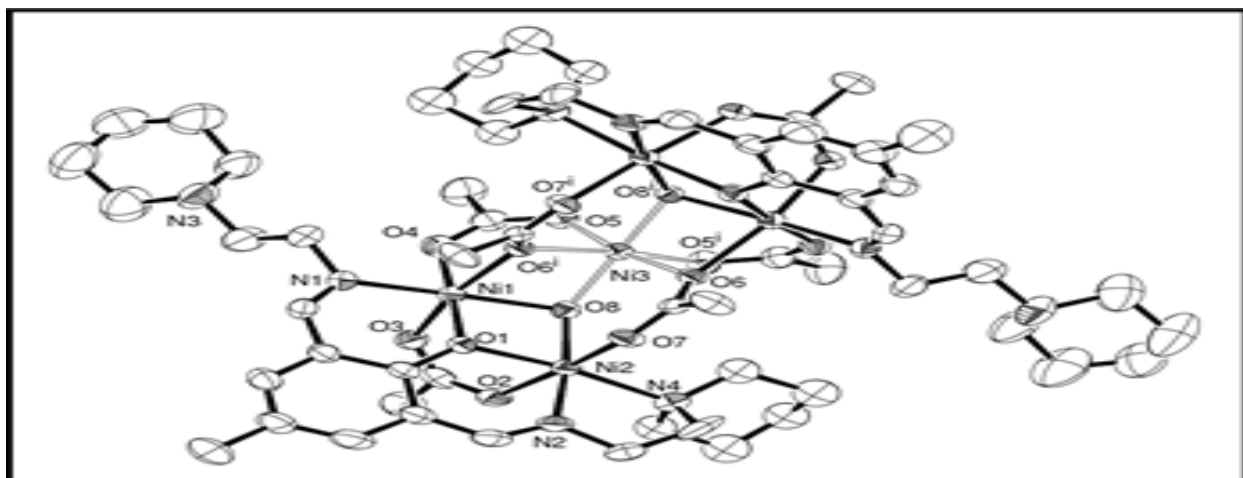


Figure 7 ORTEP drawing (35% probability ellipsoid) of the pentanuclear complex 2 of C_2 symmetry (only the coordinated atoms labeled for sake of clarity and of the disordered piperidine ring N4, only one orientation is shown).

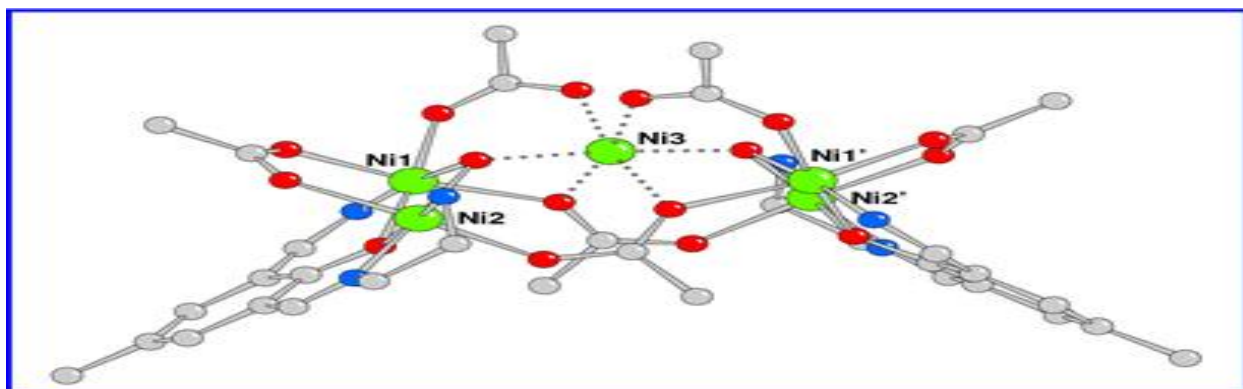


Figure 8 Side view of complex 2 (piperidine rings not shown for clarity).

Table 2 Selected bond lengths (Å) and angles (°) for complex 2.

Ni(1)-O(1)	2.029(3)	Ni(2)-O(8)	2.013(4)
Ni(1)-O(3)	2.067(4)	Ni(2)-N(2)	2.000(5)
Ni(1)-O(4)	2.050(4)	Ni(2)-N(4)	2.179(5)
Ni(1)-O(6')	2.137(3)	Ni(3)-O(8)	2.006(3)
Ni(1)-O(8)	2.034(3)	Ni(3)-O(5)	2.049(4)
Ni(1)-N(1)	2.038(5)	Ni(3)-O(6)	2.095(3)
Ni(2)-O(1)	2.035(3)	Ni(1)-Ni(2)	2.9581(10)
Ni(2)-O(2)	2.120(4)	Ni(1)-Ni(3)	3.0773(7)
Ni(2)-O(7)	2.060(3)	Ni(2)-Ni(3)	3.6227(8)

O(1)-Ni(1)-O(3)	89.69(15)	O(7)-Ni(2)-O(2)	174.85(16)
O(1)-Ni(1)-O(4)	176.27(15)	O(8)-Ni(2)-O(2)	88.66(15)
O(1)-Ni(1)-O(6')	93.75(13)	O(2)-Ni(2)-N(2)	89.48(17)
O(1)-Ni(1)-O(8)	85.09(14)	O(2)-Ni(2)-N(4)	91.75(17)
O(1)-Ni(1)-N(1)	88.61(17)	O(8)-Ni(2)-O(7)	92.17(13)
O(3)-Ni(1)-O(4)	86.61(17)	O(7)-Ni(2)-N(2)	89.20(16)
O(3)-Ni(1)-O(6')	166.38(14)	O(7)-Ni(2)-N(4)	93.01(17)
O(3)-Ni(1)-O(8)	89.24(14)	O(8)-Ni(2)-N(2)	174.23(18)

O(3)-Ni(1)-N(1)	94.98(17)	O(8)-Ni(2)-N(4)	102.86(16)
O(4)-Ni(1)-O(6')	89.96(15)	N(2)-Ni(2)-N(4)	82.7(2)
O(4)-Ni(1)-O(8)	95.29(15)	O(5)-Ni(3)-O(5')	84.6(2)
O(4)-Ni(1)-N(1)	91.27(18)	O(6)-Ni(3)-O(6')	92.83(19)
O(6')-Ni(1)-O(8)	77.94(13)	O(8')-Ni(3)-O(8)	173.98(19)
O(6')-Ni(1)-N(1)	98.27(16)	O(5)-Ni(3)-O(6)	169.85(14)
O(8)-Ni(1)-N(1)	172.40(17)	O(5)-Ni(3)-O(6')	92.01(15)
O(1)-Ni(2)-O(2)	85.85(14)	O(5')-Ni(3)-O(8)	91.08(16)
O(1)-Ni(2)-O(7)	89.15(14)	O(5)-Ni(3)-O(8)	93.38(15)
O(8)-Ni(2)-O(1)	85.47(14)	O(6')-Ni(3)-O(8)	79.54(13)
O(1)-Ni(2)-N(2)	88.95(17)	O(6)-Ni(3)-O(8)	96.26(13)
O(1)-Ni(2)-N(4)	171.29(16)	Ni(1)-O(1)-Ni(2)	93.42(14)

Primed atoms $-x+1, y, -z+1/2$.

Within the compartmental ligand the distance between Ni(1) and Ni(2) ions is 2.958(1) Å, while the intermetallic Ni(2)–Ni(3) and Ni(1)–Ni(3) separations are 3.6227(8) and 3.0773(7) Å, respectively. The longer intermetallic distance is likely induced by steric factors, since it occurs between Ni(3) and Ni(2), the latter being chelated by the imino-amino fragment. This feature has been reported also in other pentanuclear Ni clusters. Here the metals chelated by the Schiff base are a bit closer than in 1 (3.0702(7) Å), to which corresponds a Ni(1)–O(1)–Ni(2) phenoxide bridge angle of 93.42(14)° (in 1 99.35(9)°). It is plausible that the O–H groups, μ_3 -bridging the Ni₃ isosceles triangle and displaced by 0.71 Å from the metal plane, represent a key functional species beside the acetate anions, to give origin to this pentanuclear cluster.

The coordination Ni–O distances range from 2.013(4) to 2.137(3) Å, while the Ni–N bond lengths fall in between 2.000(5)–2.179(5) Å, being the longest value of the piperidine nitrogen donor. Actually compound 2 resembles the complexes reported by Fenton *et al.*, [24] which used asymmetric compartmental ligands as well as ligands bearing a carbonyl group instead of the preformed imine [25]. In all these cases the Ni₅ core has a comparable architecture, although characterized by a narrower angle between the mean planes through phenolato (54–64° to be compared with the value of 82° measured in 2). It is difficult to access if this feature is due to the different compartmental ligands or rather to packing requirements. The crystallographic analysis shows the presence of 5.5 disordered lattice water and one acetic acid molecule per complex unit. Most of these fill channels down the (101) direction formed by packing of the complexes, as shown Figure 9.

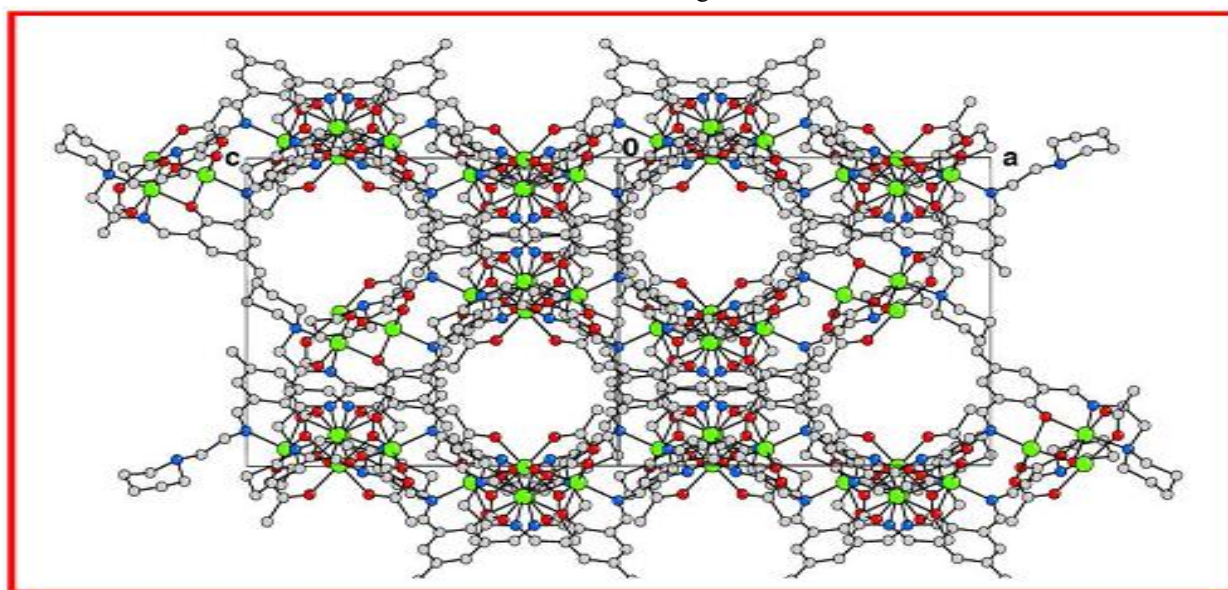


Figure 9 Crystal packing of complex 2 showing channel parallel to (101) direction.

Catechol Oxidase Activity

The ubiquitous plant enzyme catechol oxidase is a Type-3 active site copper protein where the metal ions are surrounded by three nitrogen donor atoms from histidine residues [31,32]. This protein reversibly binds dioxygen at ambient conditions and utilizes it to perform the oxidation of phenolic substrates to *o*-quinones, which later on were tested as models of catechol oxidase enzyme and in fact they can catalyze the reaction for the conversion of the 3,5-di-*tert*-butylcatechol (3,5-DTBC) to 3,5-di-*tert*-butylbenziquinone (3,5-DTBQ) that was studied in MeOH medium with the help of UV-vis spectrophotometer. The substrate 3,5-DTBC itself presents no absorption band in the region around 390 nm, but on reaction between the catalyst and the substrate in a 1:100 ratio in air saturated methanol medium, a band appeared at 390 nm and 397 nm for complex 1 and 2, respectively. Thus both the complexes are able to catalyze the formation of *o*-quinone from the catechol. Moreover the observed absorbance at 390 nm and 397 nm increased with time showing an augmented formation of quinone from catechol. For complex 2 the increase of the peak at 397 nm followed up for 60 mins is more enhanced than for 1, indicating a more rapid conversion of 3,5-DTBC to 3,5-DTBQ. On the other hand the solid state structures of the complexes (described above) suggest that complex 1 should likely favor the

conversion of 3,5-DTBC to 3,5-DTBQ to a greater extent than 2. Actually we have got just opposite result and, in order to access the apparent contradiction, we performed ESI-MS experiments to evaluate the structures of the complexes in methanol medium. Complex 1 exhibits a base peak at 724.20 amu which corroborates well with mono positive species of composition $[\text{Ni}_2(\text{L}^1)_2(\text{NO}_3)]^+$ (*m/z*, Calcd. 724.07 amu). In contrast, the analysis of ESI-MS spectrum for 2 reveals a base peak at 617.16 amu corresponding to a dinuclear species of probable composition $[\text{Ni}_2\text{L}_2(\text{OAc})_2(0.5\text{H}_2\text{O})]^+$ (*m/z*, Calcd. 616.57 amu) fractionated from the pentanuclear complex and a peak at 1331 amu related to the species having composition $[\text{Ni}_4(\text{L}^2)_2(\text{OAc})_5(\text{H}_2\text{O})]^+$ (*m/z*, Calcd. 1332.12 amu), which presents a very small percentage in methanol solution (ESI-MS spectra reported in Figure 10). Therefore, mass spectral analyses suggest that in methanol medium the pentanuclear complex 2 gets fragmented into two nickel(II) species whereas, the dinuclear entity of complex 1 remains intact. Thus, under equal molar concentrations of complexes 1 and 2, the latter generates nearly 10 times catalytically active species and consequently it shows better activity in converting 3,5-DTBC to 3,5-DTBQ. Figures 11 represent the time dependent spectral change of complexes 1 and 2, respectively upon addition of 3,5-DTBC.

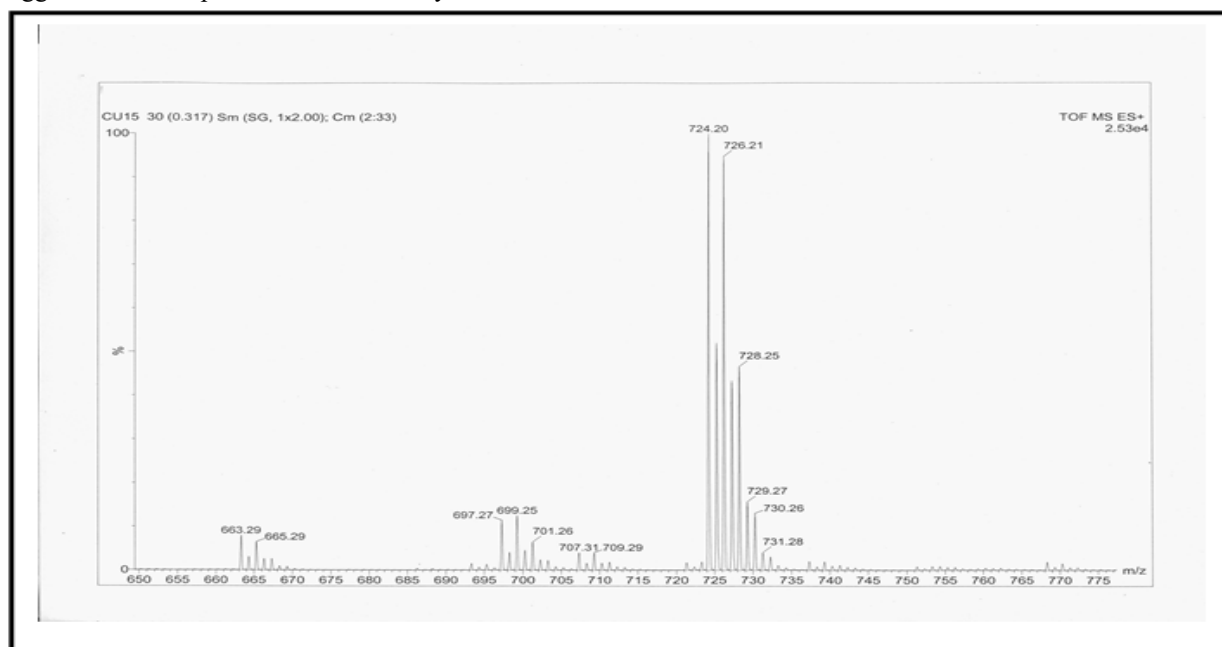
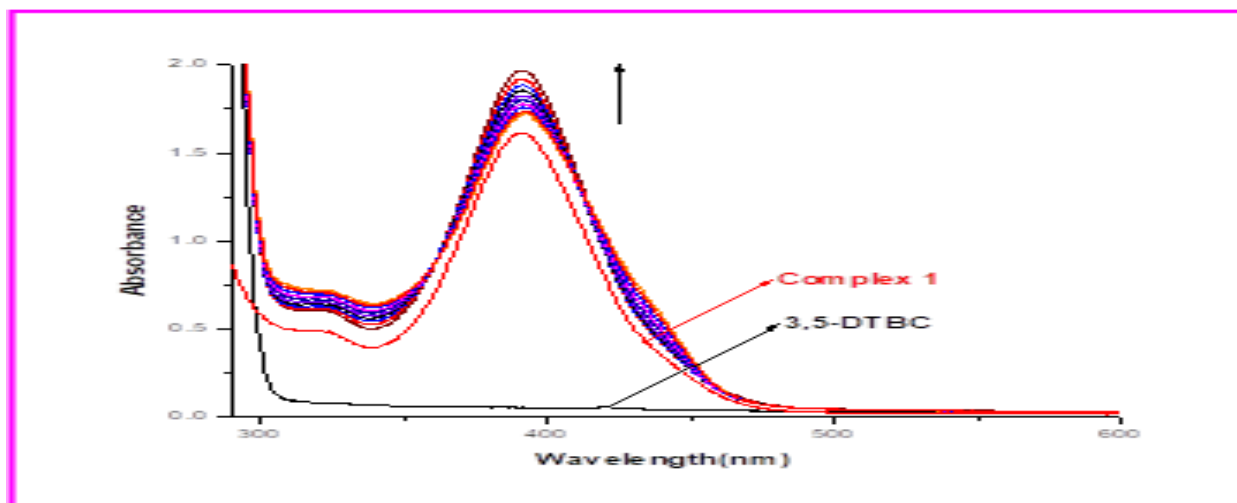
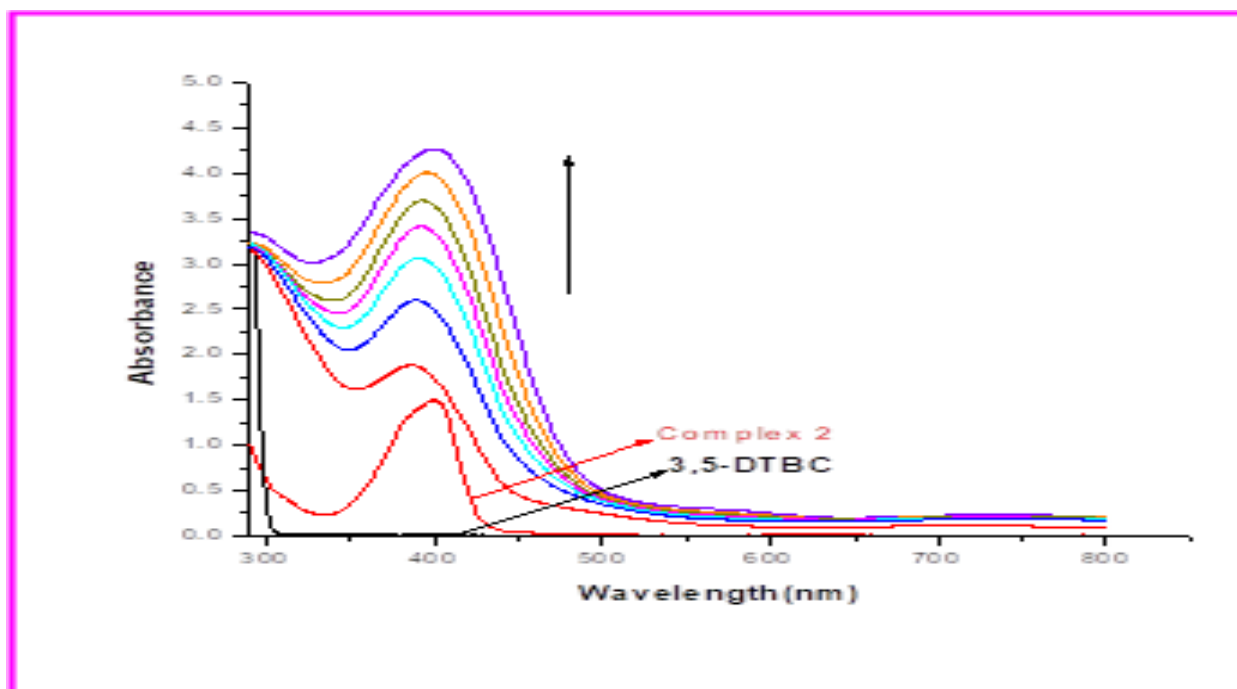


Figure 10 ESI-MS spectrum



(a)



(b)

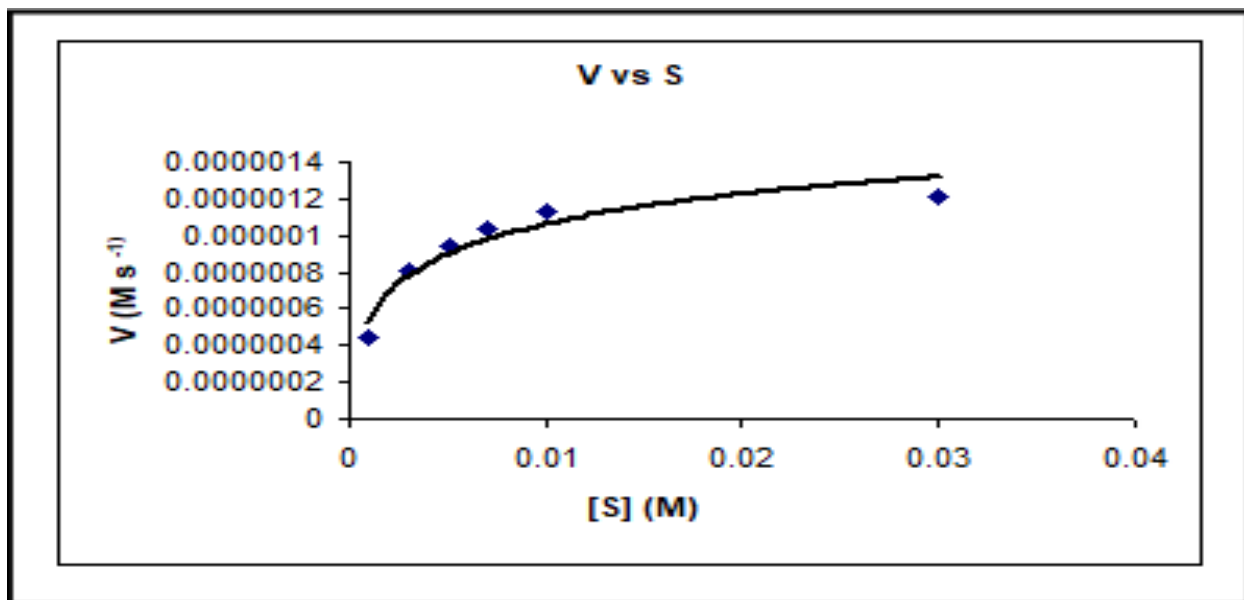
Figure 11 UV-vis spectra (300-800 nm) of (a) 1 (1×10^{-4} M) and (b) 2 (1×10^{-4} M) in methanol upon addition of 100-fold 3,5-DTBC observed at regular intervals of time.

The kinetics for the oxidation of the substrate 3,5-DTBC was determined by the initial rates method at 25 °C. The concentration of the substrate 3,5-DTBC was always kept at least 10 times larger than that of the Ni^{II} complex and the increase of 3,5-DTBQ concentration was determined in the spectral range 390 nm for complex 1 and 397 nm for complex 2. Solutions of substrate 3,5-DTBC with concentration

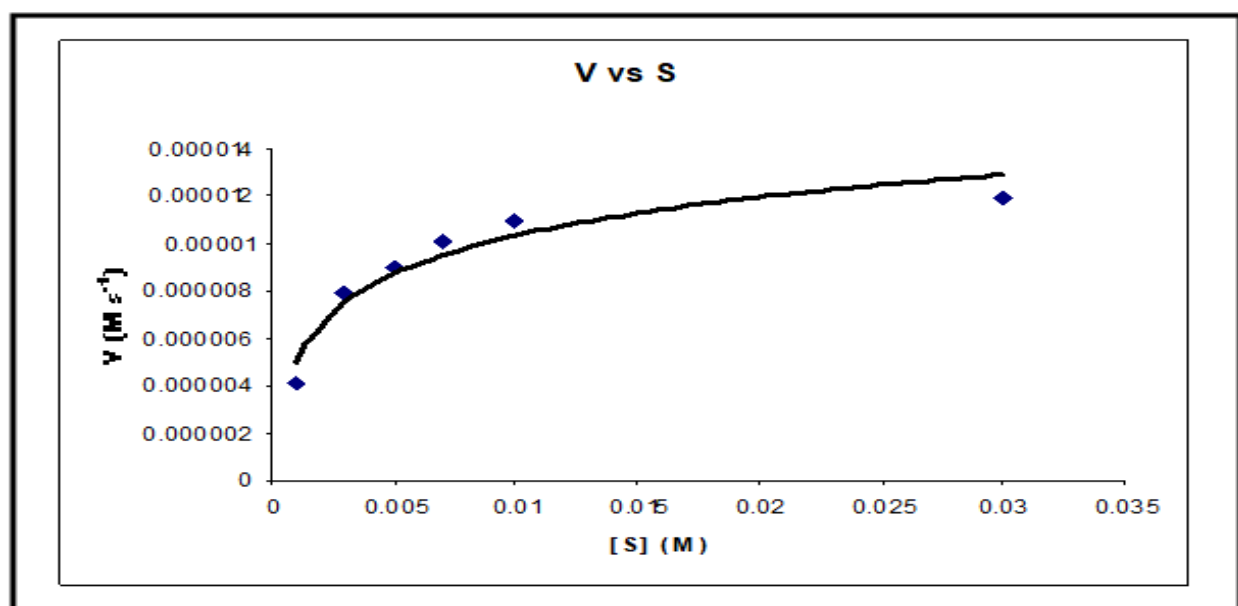
ranging from 0.001 to 0.05 mol dm^{-3} were prepared from a concentrated stock solution in MeOH medium. 2 mL of the substrate solution were poured in a 1 cm spectrophotometer quartz cell at 25 °C. Then 0.04 mL of 0.005 mol dm^{-3} Ni^{II} complex solution was quickly added to it so that the ultimate concentrations of Ni^{II} complex become 1×10^{-4} mol dm^{-3} . The dependence of the initial rate on the

concentration of substrate monitored spectrophotometrically at 400 nm are given in Figure 11. Also, here the initial rates method shows a first-order dependence on complex concentration. It is observed that complexes exhibited a considerable catecholase-type activity, by catalyzing the oxidation of the substrate DTBC to give DTBQ. They exhibited saturation kinetics at higher DTBC concentrations. For this reason, a treatment based on Michaelis-

Menten model was seemed to be appropriate. Figure 12 represents the Lineweaver-Burk plots (double reciprocal plot) for the complexes in methanol medium and it allow to evaluate different complex parameters, such as maximum velocity (V_{\max}), Michaelis binding constant (K_M), rate constant for the dissociation of substrate (i.e., turnover number, k_{cat}) in MeOH medium. The data are listed in Table 3.



(a)



(b)

Figure 11 Plot of rate vs substrate of complex 1 (a); 2 (b) 3,5-DTBC in methanol medium.

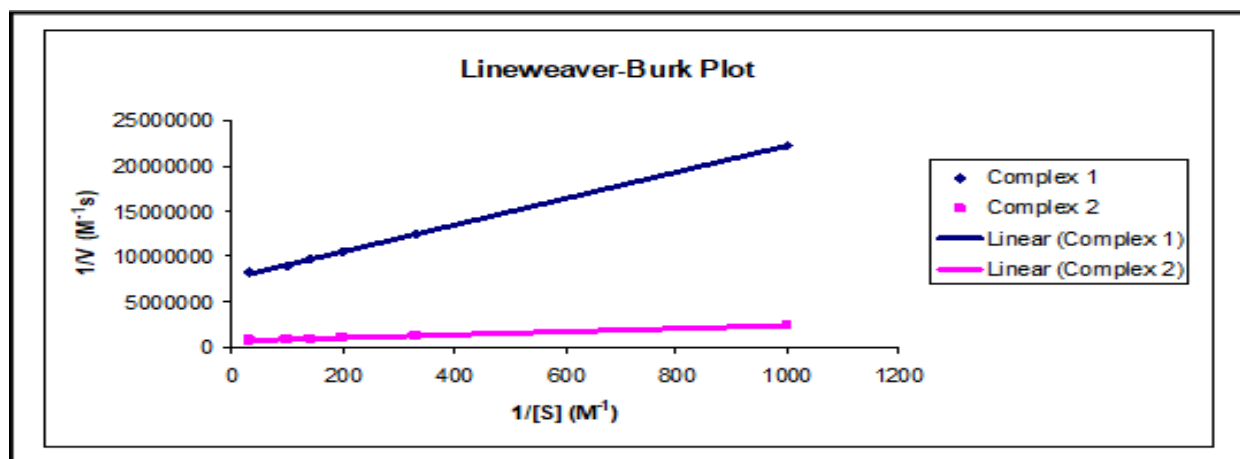


Figure 12 Lineweaver-Burk plot for complexes 1 and 2.

Table 3 Kinetic parameters of catechol oxidation catalyzed by complexes 1 and 2.

Complex	V _{max} (Ms ⁻¹)	K _m (M)	k _{cat} (h ⁻¹)
1	1.32×10^{-6}	1.93×10^{-3}	4.74
2	1.32×10^{-5}	2.21×10^{-3}	47.7

Experimental Section

Starting Materials

All chemicals were obtained from commercial sources and used as received. Solvents were dried according to standard procedure and distilled prior to use. 2,6-diethyl-4-methylphenol was prepared according to the literature method [33]. 1-(2-aminoethyl) piperidine (Aldrich), nickel(II) nitrate hexahydrate (Merck), nickel(II) acetate tetrahydrate (Loba Chemie) were purchased from commercial sources and used as received. All other chemicals used were of AR grade.

Physical Measurements

Elemental analyses (carbon, hydrogen, and nitrogen) were performed using a PerkinElmer 240C elemental analyzer. Infrared spectra (4000–400 cm⁻¹) were recorded at 300 K using a Shimadzu FTIR-8400S with KBr as medium. Electronic spectra (1500–300 nm) were obtained at 25 °C using a Hitachi U-3501 spectrophotometer in acetonitrile.

Syntheses

(a) Complex 1: $[\text{Ni}_2\text{L}_2(\text{H}_2\text{O})_4](\text{NO}_3)_2$ The complex was prepared by adding dropwise an ethanolic solution of $\text{Ni}(\text{NO}_3)_2 \cdot 6\text{H}_2\text{O}$ (0.727 gm, 2.5 mmol) over the Schiff-base formed in situ between 2,6-

diethyl-4-methylphenol and 2-(2-aminoethyl)piperidine (1:2) in anhydrous ethanol with stirring over 2 hrs and the mixture was maintained at reflux for 1 h. The mixture was filtered at its boiling point and the filtrate was evaporated at atmospheric pressure until solid started to appear. After cooling, the green precipitate was collected by filtration to give the binuclear nickel(II) complex. The binuclear nickel(II) complex was dissolved in ethanol/acetone (30 mL, 1:1) and the solution was slowly evaporated to give green single crystals of the binuclear nickel(II) complex (Figure 1(a)). Yield: 69%. Anal. Calcd. for $\text{C}_{32}\text{H}_{50}\text{N}_6\text{O}_{14}\text{Ni}_2$ (**1**): C, 44.68; H, 5.86; N, 9.77. Found: C, 44.53; H, 5.66; N, 9.62%. (b) Complex 2: $[\text{Ni}_5\text{L}_2(\text{OAc})_6(\text{OH})_2]$ The complex was synthesized by adopting a similar procedure as for **1** where $\text{Ni}(\text{OAc})_2 \cdot 4\text{H}_2\text{O}$ (0.6221 gm, 2.5 mmol) was used instead of $\text{Ni}(\text{NO}_3)_2 \cdot 6\text{H}_2\text{O}$ to give the pentanuclear nickel(II) complex (Figure 3(a)). Yield: 71%. Anal. Calcd. for $\text{C}_{58}\text{H}_{90}\text{N}_8\text{O}_{16}\text{Ni}_5$ (**2**): C, 48.08; H, 6.26; N, 7.73. Found: C, 48.01; H, 6.03; N, 7.55%.

X-ray Crystal Structure Determinations

Diffraction data for complexes **1** (at 120(2) K) and **2** (room temperature) were collected on a Bruker Smart Apex diffractometer equipped with CCD and Mo-K α radiation ($\lambda = 0.71073 \text{ \AA}$). Cell refinement, indexing and scaling of the data sets were carried out using

Bruker Smart Apex and Bruker Saint packages [34]. The structures were solved by direct methods and subsequent Fourier analyses [35] and refined by the full-matrix least-squares method based on F^2 with all observed reflections [35]. The contribution of H atoms at calculated position was introduced in the final cycles of refinement, except those of water molecules located on ΔF map and refined restraining the O-H distances at 0.85 Å. The coordinating piperidine ring (N4) in **2**, is disordered over two

conformations (occupancy of 0.50 each). Some residuals in the ΔF map were successfully refined as an acetic acid molecule (0.50 occupancy) and as four water oxygen (two at full occupancy, the other at 0.50 and 0.25 occupancy, no H atoms located). Crystallographic data and details of refinements are reported in Table 4. All the calculations were performed using the WinGX System, Ver 1.80.05 [36].

Table 4 Crystallographic Data and Details of Structure Refinements for Complexes 1 and 2.

	1	2
Empirical formula	C ₃₂ H ₅₀ N ₈ Ni ₂ O ₂₀	C ₆₀ H ₁₀₅ N ₈ Ni ₅ O _{23.50}
Formula weight	984.22	1608.07
Crystal system	Monoclinic	Monoclinic
Space group	$P 2_1/c$	$C 2/c$
a (Å)	14.5801(4)	18.1844(19)
b (Å)	10.1560(3)	15.5834(19)
c (Å)	14.0143(4)	27.789(3)
β (°)	92.4720(10)	103.798(2)
Volume (Å ³)	2073.24(10)	7647.4(15)
Z	2	4
D_{calcd} (g cm ⁻³)	1.577	1.397
μ Mo-K α , (mm ⁻¹)	0.998	1.283
$F(000)$	1028	3396
θ_{max} (°)	25.99	25.15
Reflns collected	25697	21677
Unique reflections	4078	6646
R_{int}	0.0416	0.0780
Observed $I > 2\sigma(I)$	3338	4696
Parameters	293	473
Goodness of fit (F^2)	1.047	1.043
$R1$ ($I > 2\sigma(I)$) ^[a]	0.0463	0.0607
$wR2$ ^[a]	0.1255	0.1843
$\Delta\rho$ (e/Å ³) ^[b]	1.164, -0.503	1.003, -0.561

$$^{[a]} R1 = \sum ||F_o| - |F_c|| / \sum |F_o|, wR2 = [\sum w(F_o^2 - F_c^2)^2 / \sum w(F_o^2)^2]^{1/2}$$

III. CONCLUSIONS

In summary the work demonstrates that the [1+1] or [1+2] condensed Schiff-base formations are mediated

by the anionic fragment of the nickel salts. In particular the coordination ability of acetate anions drives the synthesis towards the formation of a pentanuclear Ni₅ complex with compartmental

ligands having symmetric imine groups, while in presence of nitrates the binuclear complex obtained comprises of Schiff-base ligands with a carbonyl group instead of the preformed imine, the formation of which is likely assisted by the anion. Both the complexes exhibit catecholase-like activity in oxidizing 3,5-DTBC to 3,5-DTBQ under aerobic condition where the pentanuclear species shows better efficiency.

REFERENCES

- [1] (a) R. H. Holm, E. I. Solomon, *Chem. Rev.* 1996, 96, 7; (b) R. H. Holm, E. I. Solomon, *Chem. Rev.* 2004, 104, 2.
- [2] (a) S. J. Lippard, J. M. Berg, *Principles of Bioinorganic Chemistry*; University Science Books: Mill Valley, CA, 1994; (b) K. D. Karlin, Z. Tyeklar, *Bioinorganic Chemistry of Copper*; Chapman & Hall: New York, 1993.
- [3] A. Messerschmidt, R. Huber, T. Poulos, K. Wieghardt, *Handbook of Metalloproteins*; John Wiley & Sons: Chichester, UK, 2001.
- [4] (a) D. Gatteschi, O. Kahn, J. S. Miller, F. Palacio, *Magnetic Molecular Materials*; Kluwer Academic Publishers: Dordrecht, The Netherlands, 1991; (b) C. J. O'Connor, *Research Frontiers in Magnetochemistry*; World Scientific: Singapore, 1993.
- [5] O. Kahn, *Molecular Magnetism*; VCH: Weinheim, Germany, 1993.
- [6] (a) D. Gatteschi, R. Sessoli, *Angew. Chem., Int. Ed.* 2003, 42, 268; (b) G. Christou, D. Gatteschi, D. N. Hendrickson, R. Sessoli, *MRS Bull.* 2000, 25, 66.
- [7] (a) J. L. C. Rowsell, O. M. Yaghi, *Angew. Chem. Int. Ed.* 2005, 44, 4670; (b) L. Jiang, H. J. Choi, X. L. Feng, T. B. Lu, J. R. Long, *Inorg. Chem.* 2007, 46, 2181.
- [8] D.Y. Wu, O. Sato, C. Y. Duan, *Inorg. Chem. Commun.* 2009, 12, 325.
- [9] (a) M. Dey, C. Rao, P. K. Saarenketo, K. Rissanen, *Inorg. Chem. Commun.* 2002, 5, 380; (b) F. Luo, J. M. Zheng, M. Kurmoo, *Inorg. Chem.* 2007, 46, 8448.
- [10] E. I. Solomon, T. C. Brunold, M. I. Davis, J. N. Kemsley, K. Lee, N. Lehnert, F. Neese, A. J. Skulan, Y. S. Yang, J. Zhou, *Chem. Rev.* 2000, 100, 235.
- [11] N. A. Law, M. T. Caudle, V. L. Pecoraro, *Adv. Inorg. Chem.* 1998, 46, 305.
- [12] E. Kimura, T. Koike, S. Aoki, Yuki Gosei *Kagaku Kyokaishi* 1997, 55, 1052.
- [13] X. M. Chen, Y. Y. Yang, *Chin. J. Chem.* 2000, 18, 664.
- [14] J. H. J. Satcher, M. M. Olmstead, M. W. Droegge, S. R. Parkin, B. C. Noll, L. May, A. L. Balch, *Inorg. Chem.* 1998, 37, 6751.
- [15] P. E. Kruger, B. Moubaraki, G. D. Fallon, K. S. Murray, *J. Chem. Soc. Dalton Trans.* 2000, 5, 713.
- [16] C. J. Matthews, K. Avery, Z. Xu, L. K. Thompson, L. Zhao, D. O. Miller, K. Biradha, K. Poirier, M. J. Zaworotko, C. Wilson, A. E. Goeta, J. A. K. Howard, *Inorg. Chem.* 1999, 38, 5266.
- [17] H. Yamashita, M. Koikawa, T. Tokii, *Mol. Cryst. Liq. Cryst. Sci. Sect. A* 2000, 342, 63.
- [18] C. He, C. Y. Duan, C. J. Fang, Y. J. Liu, Q. J. Meng, *J. Chem. Soc. Dalton Trans.* 2000, 7, 1207.
- [19] F. Estevan, A. Garcia-Bernabe, P. Lahuerta, M. Sanau, M. A. Ubeda, A. M. C. Ramirez, *Inorg. Chem.* 2000, 39, 5964.
- [20] A. J. Edwards, B. F. Hoskins, R. Robson, J. C. Wilson, J. Moubaraki, K. S. Murray, *J. Chem. Soc., Dalton Trans.* 1994, 1837.
- [21] (a) A. Banerjee, R. Singh, E. Colacio and K. K. Razak, *Eur. J. Inorg. Chem.* 2009, 277. (b) C. J. Matthews, K. Avery, Z. Q. Xu, L. K. Thompson, L. Zhao, D. O. Miller, M. J. Zaworotko, K. Biradha, K. Poirier, C. Wilson, A. E. Goeta, J. A. K. Howard, *Inorg. Chem.* 1999, 38, 5266.
- [22] (a) K. Yoneda, K. Adachi, K. Nishio, M. Yamasaki, A. Fuyuhiko, M. Katada, S. Kaizaki, S. Kawata, *Angew. Chem. Int. Ed.* 2006, 45, 5459; (b) X. Feng, L. Y. Wang, J. S. Zhao, J. G. Wang, B. Liu, X. G. Shi, *Inorg. Chim. Acta* 632, 5127 ().
- [23] H. H. Monfared, J. Sanchiz, Z. Kalantari, C. Janiak, *Inorg. Chim. Acta* 2009, 362, 3791.
- [24] H. Adams, S. Clunas, D. E. Fenton, D. N. Towers, *J. Chem. Soc., Dalton Trans.* 2002, 3933.
- [25] H. Adams, D. E. Fenton, P. E. McHugh, *Inorg. Chem. Commun.* 2004, 7, 880.
- [26] H. Adams, S. Clunas, D. E. Fenton, *Chem. Commun.* 2002, 418.

- [27] D. Mandal, V. Bertolasi, J. Ribas-Ariño, G. Aromí, D. Ray, *Inorg. Chem.* 2008, 47, 3465.
- [28] K. Nakamoto, *Infrared and Raman Spectra of Inorganic and Coordination Compounds* 3rd ed.; Wiley: New York, 1978.
- [29] A. B. P. Lever, *Inorganic Electronic Spectroscopy*, 2nd ed.; Elsevier Science Publishers B.V.(Amsterdam) 1984.
- [30] B. N. Figgis, M.A. Hitchman, *Ligand Field Theory and its Application*, Wiley-VCH, 2000.
- [31] E. I. Solomon, U. M. Sundaram, T. E. Machonkin, *Chem. Rev.* 1996, 96, 2563.
- [32] E. I. Solomon, M. J. Baldwin, M. D. Lowery, *Chem. Rev.* 1992, 92, 521.
- [33] R. R. Gagne, C. L. Spiro, T. J. Smith, C. A. Hamann, W. R. Thies, A. K. Shiemeke, *J. Am. Chem. Soc.* 1981, 103, 4073.
- [34] Bruker, SMART, SAINT. *Software Reference Manual* Bruker AXS Inc. Madison, Wisconsin, USA 2000.
- [35] G. M. Sheldrick, *Acta Cryst A.* 2008, 64, 112.
- [36] L. J. Farrugia, *J. Appl. Crystallogr.* 1999, 32, 837.